Journal of Applied Polymer Science

Fabrication of a Low-Cost Nano-SiO_2/PVC Composite Ultrafiltration Membrane and its Antifouling Performance

Zhenjiang Yu,[1] Xuyang Liu,[2] Fangbo Zhao,[1,3] Xiaoyang Liang,[1] Yu Tian[3]

[1]Key Laboratory of Superlight Materials and Surface Technology, Ministry of Education, Harbin Engineering University, Harbin 150001, People's Republic of China

[2]Shale Water Research Center, 8285 El Rio St., Houston, Texas 77054

[3]State Key Laboratory of Urban Water Resource and Environment, Harbin Institute of Technology, Harbin 150090, People's Republic of China

Correspondence to: F. B. Zhao (E-mail: zfbhit@163.com)

ABSTRACT: A novel low-cost SiO_2/Polyvinylchloride (PVC) membrane with different nano-SiO_2 particles loading (0–4 wt %) was prepared by the phase-inversion process. The optimum nano-SiO_2 dosage was determined as 1.5 wt % based on the casting solution compositions, the membranes' mechanical properties and hydrophilicities, the pure water fluxes, microstructures, and absorption of protein. Compared with the bare membrane, the membrane with 1.5 wt % nano-SiO_2 addition presented better capabilities against the protein absorption and bacterial attachment, better antifouling performance, and higher flux recovery ratio in filtration of the supernatant liquor which collected from a secondary sedimentation tank in a municipal wastewater plant. The SiO_2/PVC membranes have applicable potential in the municipal wastewater treatment for their low price, good antifouling performance and high removal efficiencies of SS (over 97.2%), COD (up to 82.9%) and total bacteria (more than 93.6%). © 2014 Wiley Periodicals, Inc. J. Appl. Polym. Sci. **2015**, *132*, 41267.

KEYWORDS: composites; hydrophilic polymers; membranes; nanoparticles; separation techniques

Received 12 April 2014; accepted 21 July 2014
DOI: 10.1002/app.41267

INTRODUTION

Ultrafiltration separation technology has received increased attention for concentration, purification, and separation of various products in food, medical, biotechnology, papermaking, and dairy industry.[1,2] For most of the commercial ultrafiltration membranes, polymeric materials, including polyvinylidene fluoride (PVDF), polyethylene (PE), polysulfone (PSF), polyethersulfone (PES), and polypropylene (PP), have been commonly chosen as the backbone materials. Backbone materials have a great contribution to the cost of the membranes, which is a determining factor for the extensive application of membranes, especially in the developing countries. Compared with other commonly used backbone materials, polyvinylchloride (PVC) exhibits robust mechanical strength, low-cost, and other excellent physical and chemical properties such as high resistance to acids, bases, solvents, and chlorine.[3–5] Although PVDF membranes also have excellent performance and extensive application, PVC is considerably cheaper than PVDF (<1/10 price), and PVC-based membranes can be successfully used in some ultrafiltration separation fields.[6,7]

However, researches on PVC membrane fabrication are not sufficient. The main disadvantage of PVC-based membrane involves its inherent hydrophobic character, which always leads to a high fouling tendency in some sewage treatments. Membrane fouling often results in the loss of filtration flux, high energy cost, deterioration of effluent quality and frequent membrane cleaning.[8] Previous researches have reported that various types of contaminants in the feed, including inorganic (clays and mineral particles), biological (bacteria, fungi), and organic (oils and humics), can cause membrane fouling.[9] It is generally accepted that increasing the hydrophilicity of the membrane surface is an effective method to mitigate the membrane fouling.[10] Thus, it is an urgent need to develop the hydrophilicity of the PVC-based membranes for enhancing their antifouling performance.

Many modified methods, including the physical blending, chemical grafting, and surface modifications, have been recently investigated.[11–15] Among them, blending polymer with inorganic materials achieves high hydrophilicities and strong antifouling membranes, and meanwhile keeps excellent mechanical property and permeability.[16–18] Varieties of inorganic materials such as alumina (Al_2O_3),[19] titanium dioxide (TiO_2),[20,21] zirconium (ZrO_2),[22] silica (SiO_2),[18,23,24]and multi-walled carbon nanotubes (MWCNTs)[25,26] have been used to fabricate inorganic–polymer composite membranes. Among these materials, silica is the most conveniently and commonly used because of

Table I. Compositions of PVC Membrane Casting Solutions

Membrane	PVC (%)	SHMP (%)	DMAC (%)	PVP (%)	Nano-SiO_2 (%)
M-0	12	1.5	82.5	4	0
M-1	12	1.5	82.5	4	1
M-1.5	12	1.5	82.5	4	1.5
M-2	12	1.5	82.5	4	2
M-3	12	1.5	82.5	4	3
M-4	12	1.5	82.5	4	4

its inert reactivity, well-known chemical properties, low price and mature prepare process.[27,28] Furthermore, the structure of abundant Si—OH groups exhibits great hydrophilicity and other favorable properties. For instance, Adams et al.[29]found that mixed nanosized SiO_2 at 5000 ppm resulted in 99% growth reduction of *B. subtilis*, and thus, exhibit better antifouling performance. Jin et al.[30] found that the addition of nano-SiO_2 in the skin layer could improve the thermal stability, hydrophilicity and permeation property of the membrane without sacrificing its rejection rate. In addition, the nano-composite NF membrane exhibited better performance in treating acidic feeds and separating salt solution containing bivalent anions. Yu et al.[31]reported the significantly improvement of the surface hydrophilicity and permeation properties with the addition of the SiO_2@N-Halamine to membranes. Moreover, hybrid membranes also showed superior antifouling and antibacterial performance. However, few literatures reported the identification and application of nano-SiO_2 particles as the modified additives to PVC-based membranes.

In this study, PVC membranes modified with different nano-SiO_2 particles loading are prepared and characterized. The optimal amount of the additives is determined to achieve the best performance. Also, their antifouling performance and retention abilities are investigated with multiple absorption and filtration experiments.

EXPERIMENTAL

Materials

The polrvinylchloride (PVC, $M_w = 80{,}000$ g mol^{-1}, Shenyang Chemical Industry, China) resin was used as the membrane backbones material. *N*,*N*-dimethylacetamide (DMAC, AR, Bodi, China) was employed as the PVC solvent. Commercially available Silica (SiO_2) nano-sized particles with a diameter of about 15 nm (Hangzhou Wanjing New Material, China.) were added into PVC casting solutions. Other additives included Sodium Hexameta Phosphate (SHMP, AR, Fuchen, China) and polyvinylpyrrolidone (PVP, AR, Lanji, China) which were utilized as the dispersing and pore-forming agent, respectively. Bovine serum albumin (BSA, $M_w = 67{,}000$, Shanghai Bio Life Sci. and Tech., China) was utilized in protein adsorption experiment. Polyethyleneglycol ($M_w = 6000$ g mol^{-1}, $M_w = 20{,}000$ g mol^{-1}, Sinopharm Chemical reagent, China) and poly (ethylene oxide) ($M_w = 100{,}000$ g mol^{-1}, $M_w = 300{,}000$ g mol^{-1}, Aladdin Industrial Corporation, China) were utilized to obtain the molecular-weight cut-off values of membranes. The supernatant liquor for filtration test was collected from a secondary sedimentation tank of Wenchang sewage treatment plant in Harbin, China. Ultrapure water (Milli-Q Academic A10, Millipore, USA) was used for all the experiments.

Membrane Preparation

Preparation Process. SiO_2/PVC composite membranes were synthesized using the wet-phase inversion process. First, nano-SiO_2 particles were dispersed into DMAC in an ultrasonic bath at 40 kHz for 20 min at room temperature, which facilitated the dispersion of the nano-SiO_2. PVC resin and PVP were slowly added into the solution followed by a 24 h stirring at 25°C. The compositions of the casting solutions are shown in Table I.

The homogeneous cast solutions were then sealed and stored at 25°C for 24 h to remove air bubbles. Then the casting solution was casted onto a clean glass plate using a membrane maker with a thickness of 500 μm. After being left on the glass plate for 15 s, the cast polymer film was immersed into a coagulation bath (ultrapure water at ambient temperature). After complete coagulation, the formed membrane was transferred to another ultrapure water bath and immersed for 48 h to remove the residual DMAC.

TEM and FTIR Analyses of the Nano-SiO_2 Particles. The microstructures and distributions of the nano-SiO_2 particles were analyzed by transmission electron microscopy (TEM, JEM-2000EX, Japan) to identify their mean grain size. Before testing, the nano-SiO_2 particles were scattered in alcohol. The completely dry nano-SiO_2 particles were tested using a NEXUS 670 Fourier transform infrared spectroscopy (FTIR, PE-100, USA) to determine the chemical structures of the particles.

Properties Analyses of the Casting Solutions. The viscosities of different casting solutions were tested by a rotational viscometer (NDJ-5S, Shanghai Changji Instrument, China) at 25°C. Every sample was tested four times at least. The appearance of different casting solutions was characterized by a high-resolution digital camera.

Membrane Characterization

To determine the effect of nano-SiO_2 added into PVC-based membrane and the optimum dosage amount, various characterization methods were performed.

1. Membrane thickness was identified through a film thickness analyzer (CH-1-S, Shanghai Liuling, China) after the samples were dried at room temperature. Each membrane sample was analyzed eight times at different positions.

2. Membrane mechanical property was measured with an electric elastic yarn strength analyzer (YG020B, Nantong Sansi, China). The measurements were performed at room temperature and the rate of pull was 2 mm min^{-1}. Every membrane sample was tested at least four times.
3. Membrane permeation flux was analyzed by dead-end filtration of ultrapure water with a stirred cell unit (Model8200, Millipore, USA) at 0.1 MPa. Before testing, membrane sample was preload at 0.2 MPa for 10 min.
4. The contact angle (CA) of water on membrane was directly measured with a JYSP-360 contact angle goniometer (Jin Shengxin, China) and every specimen was measured 8 times at different positions.
5. The membrane porosity (%) was calculated according to the method of dry-wet weight. Mean pore radius was determined by using the filtration velocity method as stated in the Guerout–Elford–Ferry equation.[32] The same dead-end filtration unit was fed with Poly(ethylene oxide)(PEO) or Polyethyleneglycol (PEG) of different molecular weights that is, $PEO_{100,000}$ and $PEO_{30,0000}$, $PEG_{6,000}$, $PEG_{20,000}$, in order to obtain the molecular-weight cut-off values of membranes. The concentrations of both the feed water and the permeation water were determined using total organic carbon analyzer (TOC-VCPN, Shimadzu Corporation, Japan).
6. Membrane cross-section morphology was analyzed by a scanning electron microscope (SEM, S-4700, Hitachi, Japan) at 10 KV in a high vacuum mode after coating with ~10 nm of gold to observe membrane asymmetry and pore structure. The cross-section of membranes was obtained by breaking the membranes in liquid nitrogen. At the same time, Energy Dispersive Spectrometer (EDS) was used to check whether the nano-SiO_2 particles were inlaid on the membranes.

Membrane Antifouling Experiment

Protein Static Absorption Experiment. Protein solutions of 1.0 g L^{-1} BSA were freshly prepared by dissolving BSA into 0.1*M* phosphate buffer solution (PBS, pH = 7.4).[33,34] Membrane samples with the diameter of 1.5 cm were immersed into six-well plate filled with 5 mL protein solutions. Then the samples were incubated at 25°C for 2 h to attain equilibrium. The protein concentrations before and after the absorption were obtained through UV spectrophotometer (TU-1810, Beijing Purkinje Genera, China) at wavelengths 280 nm and the absorption amount was calculated by comparing the absorption intensity variation. Each test was performed three times on separate membrane sample.

***E. coli* Absorption Experiment.** Cultures with 1 mL *E. coli* bacteria suspension were incubated at 37°C and shaken at 130 rpm lasted for 12 h. Subsequently, the membrane samples were immersed into a six-well plate filled with 5 mL bacterial suspension and incubated at 37°C lasted for 3 h. Then the membrane samples were washed with PBS buffer for three times at 37°C. All the washing fluid was collected and then 1 mL solution was taken out for further expanded culture on a solid plate culture medium. Bacteria attached on the sample surfaces were sought by SEM.[33]

Ultrafiltration Separation of the Supernatant Liquor. Fouling experiments were performed in the dead-end filtration system utilizing the supernatant liquor as the feed solution. To verify the long-term antifouling performance of membranes, multicycle operations were performed. Each filtration cycle consisted of two stages: fouling and physical cleaning.[35] In this study, the constant value of the pure water flux of the membrane was defined as J_W. The constant permeation flux value of the feed water was denoted as J_P. Additionally, the physical cleaning process was carried out as follows. First, the fouled membrane was intensively washed using the ultrapure water. Then the membrane would filter ultrapure water at 0.2 MPa for 10 min after inverting its filtration layer. After four filtration cycles, the pure water flux was measured again and its steady value was recorded as J_R.

The flux recovery ratio (FRR) and the relative flux reduction (RFR) were calculated according to the following eqs. (1) and (2)[36]:

$$FRR(\%) = \frac{J_R}{J_W} \times 100\% \quad (1)$$

$$RFR(\%) = \left(1 - \frac{J_P}{J_W}\right) \times 100\% \quad (2)$$

In addition, the water quality of the feed and permeation water were further assessed. In this study, suspended solids (SS), chemical oxygen demand (COD) and total bacterial amount were chosen as the evaluation indexes. And every water sample will be tested in triplicate.

RESULTS AND DISCUSSION

Properties of the Casting Solutions

As shown in Figure 1(a), the size of spherical nano-SiO_2 particles arranges from 15 to 20 nanometers (nm). Figure 1(b) introduces the FTIR spectra of the completely dry nano-SiO_2 particles. Peaks at 1106 and 802 cm^{-1} correspond to asymmetric and symmetric Si—O—Si stretching, respectively. The peak at 3430 cm^{-1} corresponds to the stretching vibration absorption of —OH. These characteristic peaks reflect that the nano-SiO_2 particles presented good hydrophilicities.

The viscosities of PVC casting solutions with different nano-SiO_2 loading are depicted in the Figure 2(a). An increase in casting solution viscosity was observed with the addition of nano-SiO_2 particles. The viscosities of the casting solutions showed a sharp increase when the nano-SiO_2 loading was more than 2 wt %. A maximum value of the solution viscosity was noted with the highest loading of nano-SiO_2, i.e. 4 wt %. Majeed et al.[37] also reported the similar results in their published research.

Figure 2(b) implies the appearance of the PVC casting solutions. It was found that there still existed some residual air bubbles in the casting solutions with the loading of nano-SiO_2, i.e., 3 or 4 wt %, even after degassing treatment for 24 h. This phenomenon might have a positive connection with their high viscosities. Generally, the casting solution with high viscosity always presents a bad degassed effect. The residual air bubbles can result in defects in the membrane during preparation. Also, the high viscosity can cause the worse rheological property. Therefore, the addition of SiO_2 needs to be properly controlled in a reasonable extent.

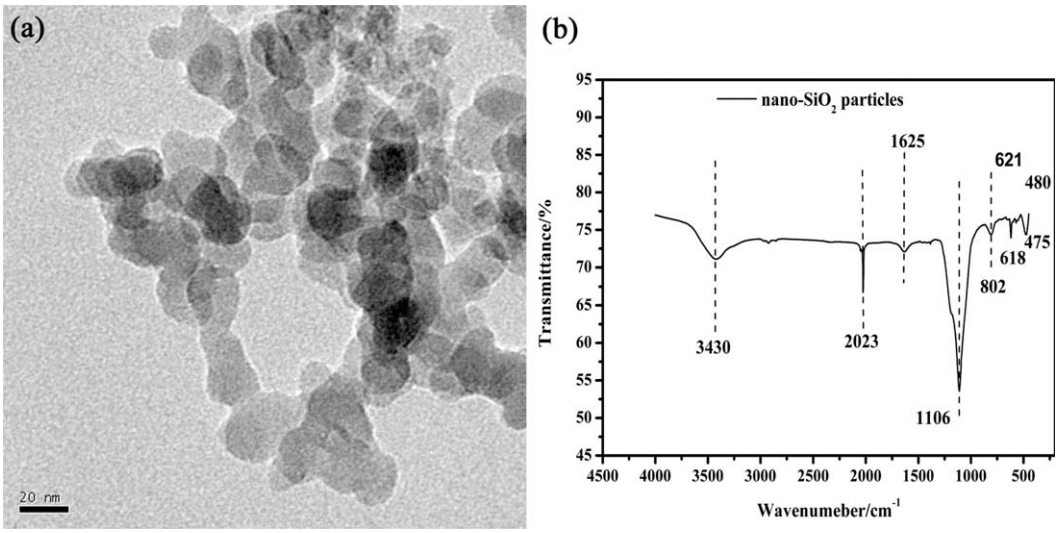

Figure 1. TEM image of purified nano-SiO_2 (a) and FTIR spectra of completely dry nano-SiO_2 particles (b).

Mechanical Properties of the Modified Membranes

The results of tensile strength and elongation at break tests are shown in Table II. Both of them increased with the nano-SiO_2 addition and then reached a maximal value when the dosing amount was 1.5 wt %, indicating the reinforcement effect of nano-SiO_2 on mechanical strength. Specifically, compared with the unmodified membrane, the tensile strength of the membrane blended with 1.5 wt % nano-SiO_2 increasedof 41.46%. The addition of the nano-SiO_2 inorganic particles to the PVC organic polymer solution helps to bridge the polymer chains thanks to their high surface energy. Consequently, the mechanical properties of the organic-inorganic membranes can be enhanced. But the mechanical properties presented a significant decline when the concentration of nano-SiO_2 reached higher value e.g. 4 wt %. It is noticed that when the concentration of nano-SiO_2 particles was more than 2%, there were some residual air bubbles, which is difficult to be removed from the casting solution even after they were degassed for a very long time [Figure 2(b)]. Thus, one possible reason of the reduced mechanical properties may result from the residual air bubbles which can lead to the defects of the fabricated membranes. This phenomenon reveals that the appropriate addition of nano-SiO_2 particles can improve the membrane mechanical property. Meanwhile, the concentration of the nano-SiO_2 particles should be controlled considering the degassed effect of the casting solution.

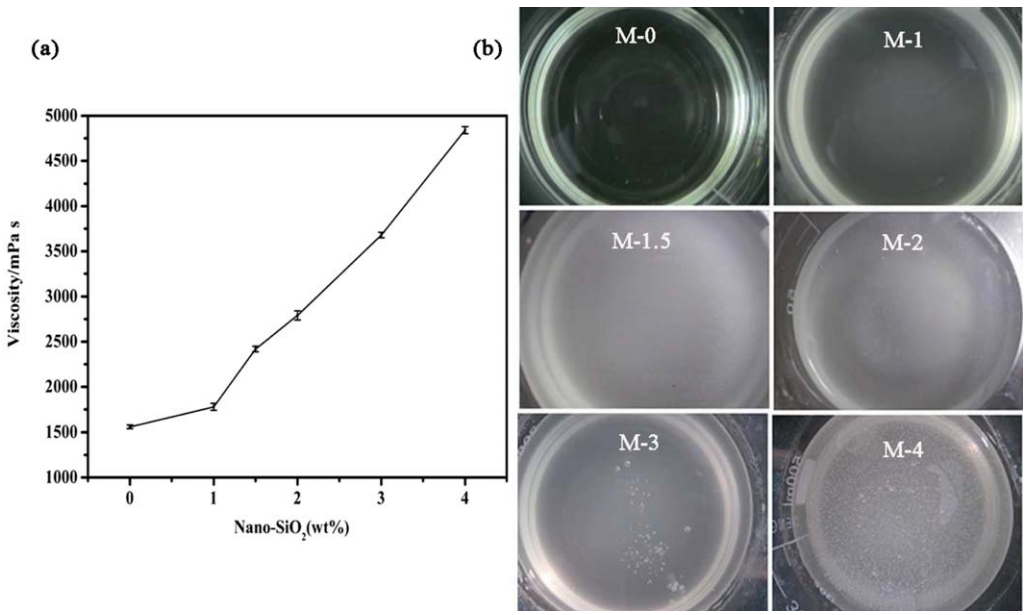

Figure 2. Viscosities of PVC solutions with different nano-SiO_2 loading (a) and the appearance of the casting solutions (b). [Color figure can be viewed in the online issue, which is available at wileyonlinelibrary.com.]

Table II. Properties of SiO_2/PVC Membranes with Different Nano-SiO_2 Loading

	Thickness (μm)	Tensile strength (cN)	Elongation at break (%)	CA (°)	PWF (L m^{-2} h^{-1})[a]
M-0	425.5 ± 16.5	269.78 ± 10.2	13.78 ± 0.80	79.67 ± 1.1	199
M-1	506.0 ± 18.8	348.33 ± 8.6	23.91 ± 1.2	67.97 ± 1.4	217
M-1.5	570.5 ± 11.1	381.63 ± 7.5	31.20 ± 0.76	61.38 ± 1.3	232
M-2	610.5 ± 17.6	380.10 ± 4.6	27.28 ± 1.1	60.05 ± 2.0	233
M-3	692.4 ± 9.3	377.63 ± 4.8	20.10 ± 0.56	61.45 ± 2.2	230
M-4	822.1 ± 15.4	324.11 ± 5.3	14.09 ± 1.65	62.74 ± 2.4	-

[a] Note: the PWF of the membrane was tested under 0.1 MPa.

Hydrophilicities of the Membranes

As depicted in Table II, the contact angle (CA) values presented conspicuous decrease tendency when more nano-SiO_2 were added within the dosage range. For example, the CA value of M-1.5 decreased from 79.67° (control sample) to 61.38°, about 22.96% of decrease. But the CA values exhibited a significantly decline when the concentration of SiO_2 was more than 2 wt %. These results were similar to the previous publications.[11,38] This phenomenon could be attributed to the hydrophilic functional groups such as Si—OH on the surface of nano-SiO_2 particles [Figure 1(b)]. When they were blended with the PVC resin, nano-SiO_2 particles would be uniformly inlaid on the membranes' surface and result in the improvement of the hydrophilicities.

Fluxes of the Membranes

A slight increase in PWF was found with the increase of SiO_2 concentration (Table II). The flux of M-1.5 was 16.6% higher than the control sample. Nevertheless, the flux of M-4 could not be measured because of the existence of the pinhole defects on the membrane sample. The increased fluxes of the modified membranes (e.g., M-1.5) mainly resulted from the improved hydrophilicity of the modified membrane surface, which decreased the resistance of the water filtration through the membrane.

Porosity, Mean Pore Radius, and Molecular-Weight Cut-Off Values of Membranes

Figure 3 shows that the porosity, mean pore radius, and molecular-weight cut-off values of different membranes. It was found that the mean pore size displayed a slight decline with the increase of nano-SiO_2 loading [Figure 3(a)]. But an obvious increase in porosity was observed with the addition of nano-SiO_2 [Figure 3(a)]. It can be interpreted as this: with the addition of the nano-SiO_2 particles into the PVC casting solutions, the chain segment of the polymer cannot spread during membrane formation, which causes the diminished pore size.[18] Meanwhile, more gaps might be produced between the hydrophilic groups on nano-SiO_2 and the hydrophobic PVC chains, which are help to form a more porous structure. In addition, the decrease in the mean pore size may be responsible for the increase of retention properties [shown in Figure 3(b)]. Both the modified and unmodified membranes present a high rejection ratio of $PEO_{100,000}$ (up to 90%). According to the molecular-weight cut-off value of membrane, the membrane prepared in our work can be defined as 100 kDa.

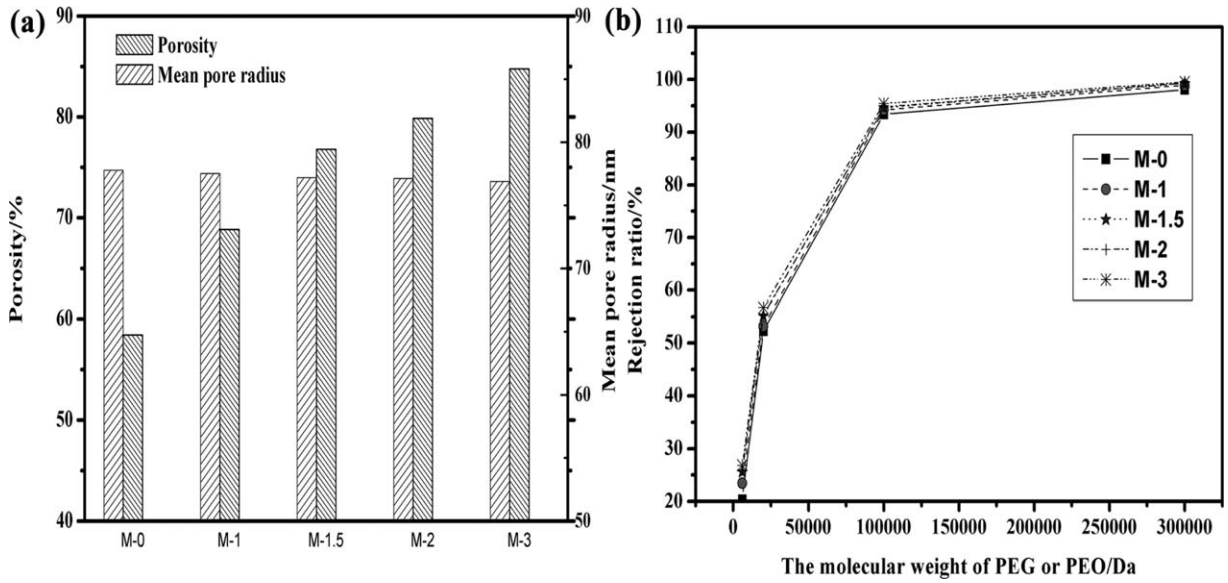

Figure 3. Porosity, mean pore radius, and molecular-weight cut-off values of different membranes.

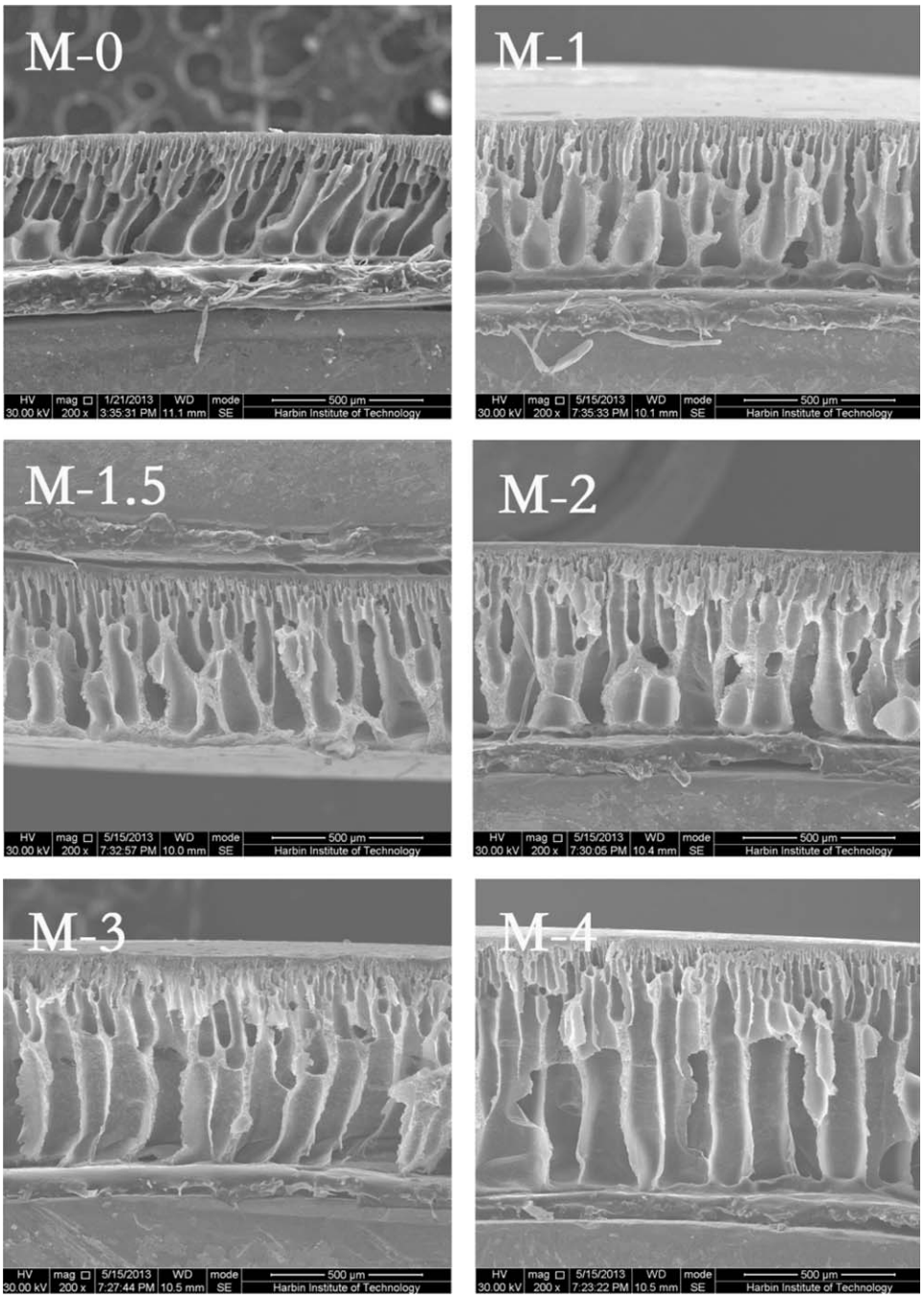

Figure 4. SEM images of cross-section of different SiO_2/PVC membranes: all the magnification is ×200 and all the scale bar is 500 μm.

Micro-Structure Analyses of the Membranes

Figure 4 shows the SEM images of the unmodified and modified membranes' cross-section structures. The pores with typical asymmetric morphology are clearly observed in all the images. There is a thin and compact filtration layer on the top of the membrane, and a thick and loose supporting layer with a large amount of macro-voids at the bottom. This phenomenon indicates that the addition of the nano-SiO_2 particles did not change the asymmetric structures of the membranes' cross-sections.

Nonetheless, from the top layers of the cross-section images, the thickness of the top layer increased with the increasing concentration of the nano-SiO_2 particles. The top layer mostly acts as the filtration layer in the membrane separation process. Consequently, the addition of nano-particles may improve the retention ability of the modified membrane. It can be interpreted as follows: with the addition of nano-SiO_2 particles, the viscosity of the nano-SiO_2/PVC polymer casting solution increased clearly [Figure 2(a)], which probably reduced the diffusion rate of the solvent and non-solvent and lead to thicker and compact top

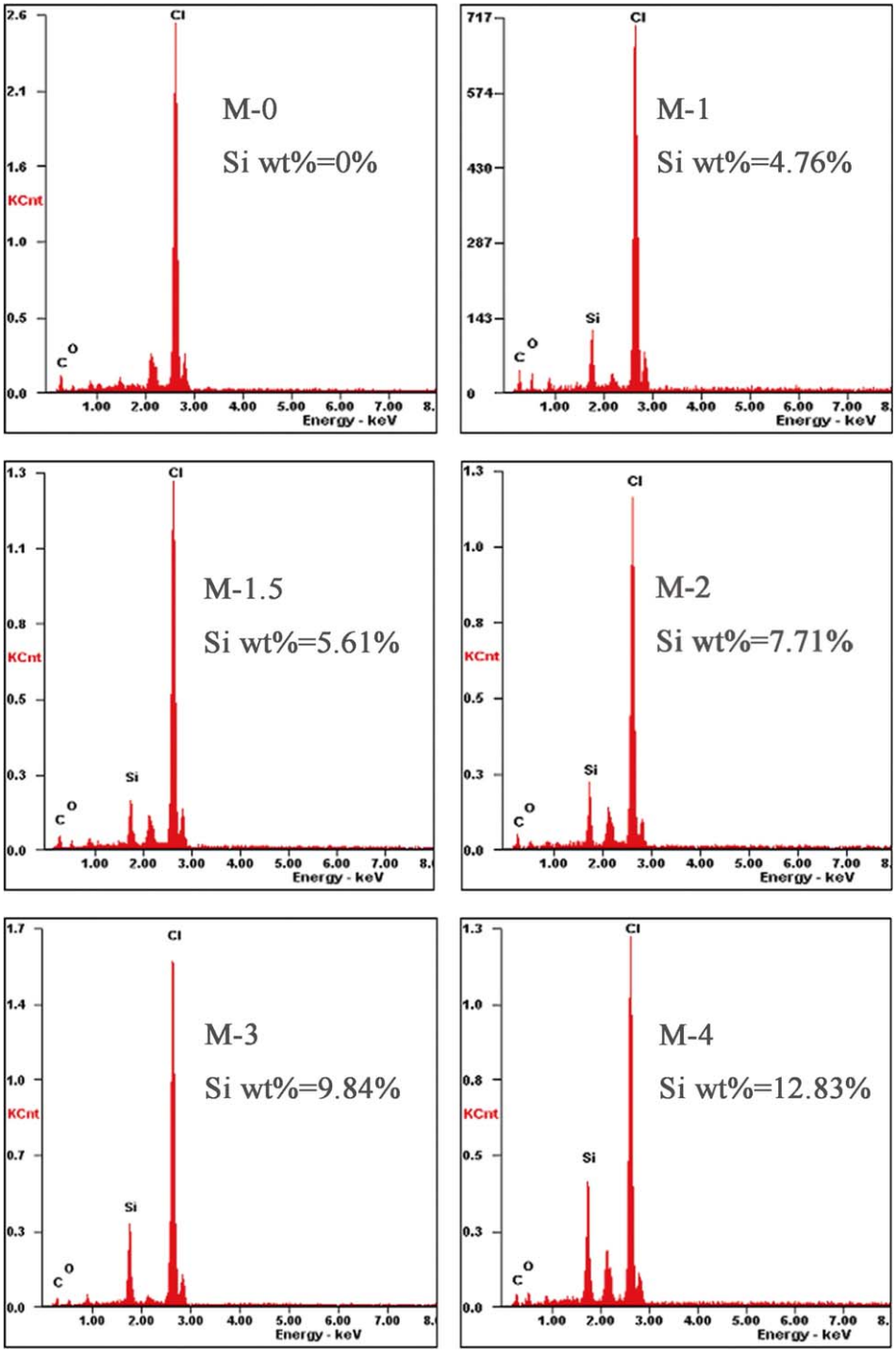

Figure 5. EDS analyses of different SiO_2/PVC membranes. [Color figure can be viewed in the online issue, which is available at wileyonlinelibrary.com.]

layer of membrane. In addition, membrane thickness was also increased with the nano-SiO_2 loading (Figure 3) and reached the maximal value of 822.1 μm for M-4 (Table II), which was attributed to the increased viscosities of casting solutions.

EDS Analyses of the Membranes

Compared with the unmodified membrane, it was found that the EDS analyses of the modified membranes contained obvious silicon and oxygen element characteristic peaks (depicted in Figure 5). These characteristic peaks indicated the successful incorporation of nano-SiO_2 particles. Meanwhile, the intensity of silicon peak was enhanced by the increase of nano-SiO_2 concentration, which indicated that more silica had been accumulated in the skin layer. These phenomena verified that it was the nano-SiO_2 that improved the hydrophilicities of PVC materials.

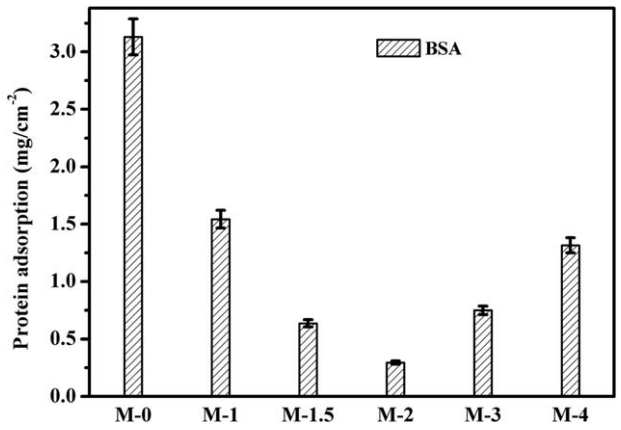

Figure 6. Absorption of protein on different SiO_2/PVC membranes.

Membrane Antifouling Analysis

Protein Static Absorption Analysis. Previous studies showed that even a small amount of protein adsorption on membrane surface resulted in the propagation of unfavorable bio-fouling and bio-film formation.[39,40] As shown in Figure 6, all the modified membranes exhibited lower protein absorption than the unmodified one. A minimum protein adsorption amount was observed when the loading of nano-SiO_2 was 2 wt %. The hydrophilicity and roughness of the membrane surfacemight be positively associated with the protein adsorption amount. The membrane marked M-2 exhibited the best hydrophilicity (Table II) and appropriate roughness. However, a higher dosage of the nano-SiO_2, i.e. 3%, 4%, lead to a much rougher surface[38] and decreased hydrophilicity of the modified membrane (Table II). That's the reason for a slight increased tendency of protein adsorption amount at a nano-SiO_2 loading rate of larger than 2%.

With comprehensive consideration of the properties of casting solution, mechanical properties, pure water flux, hydrophilicities, microstructures, and protein absorption on the different SiO_2/PVC membranes, the optimum nano-SiO_2 dosage was determined as 1.5 wt %. Thus, the membrane with 1.5 wt % nano-SiO_2 was applied as the representative of the modified membranes for the further study.

***E. coli* Absorption Analysis.** Figure 7 clearly showed that there was fewer *E. coli* attached to the modified membrane [Figure 7(c,d)] in contrast with the unmodified membrane [Figure 7(a,b)]. Specifically, there were only 12 CFU mL^{-1} *E. coli* communities in the washing fluid collected from the modified

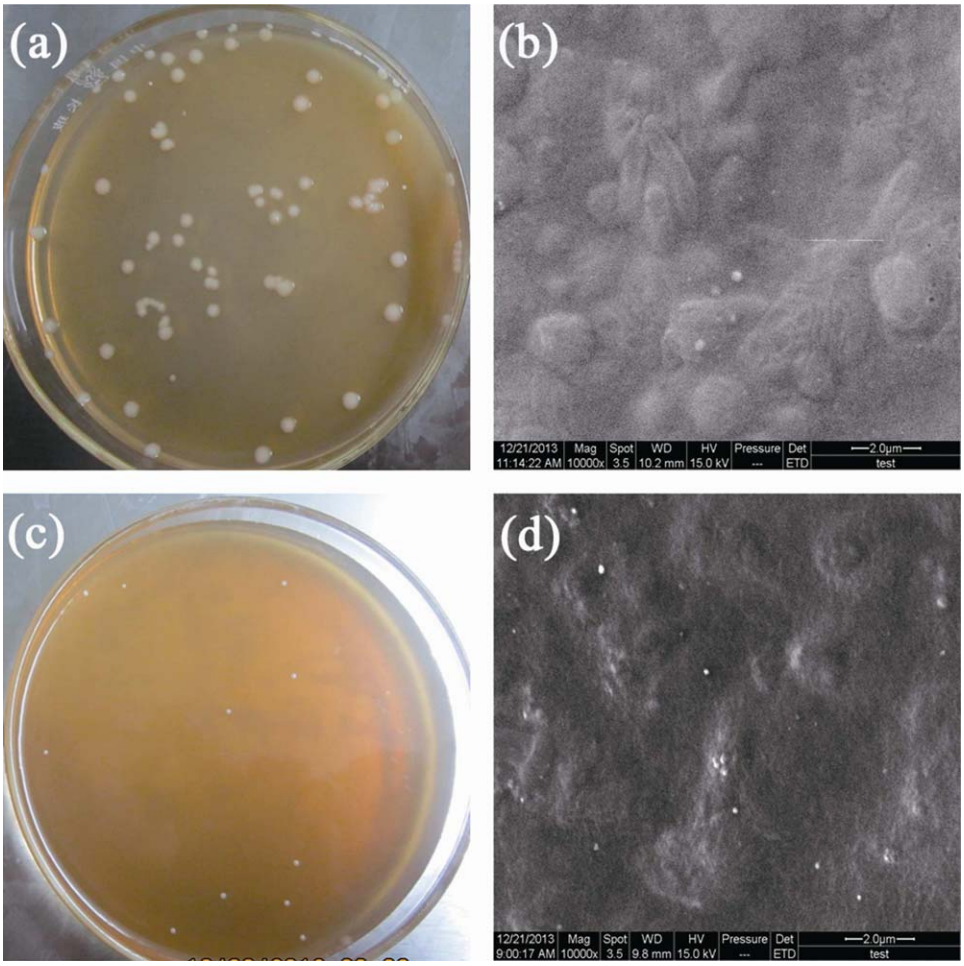

Figure 7. Colonies formed on culture by the *E. coli* from the unmodified (a) and modified membrane surface (c); and SEM images of the unmodified (b) and modified membrane (d) after *E. coli* attachment. [Color figure can be viewed in the online issue, which is available at wileyonlinelibrary.com.]

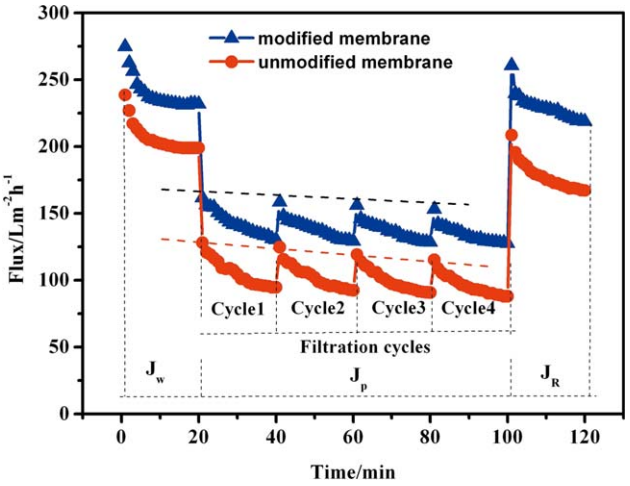

Figure 8. Flux variations of different membranes in the four filtration cycles: the traces of the initial flux in each cycle for different membranes were portrayed using dashed lines. [Color figure can be viewed in the online issue, which is available at wileyonlinelibrary.com.]

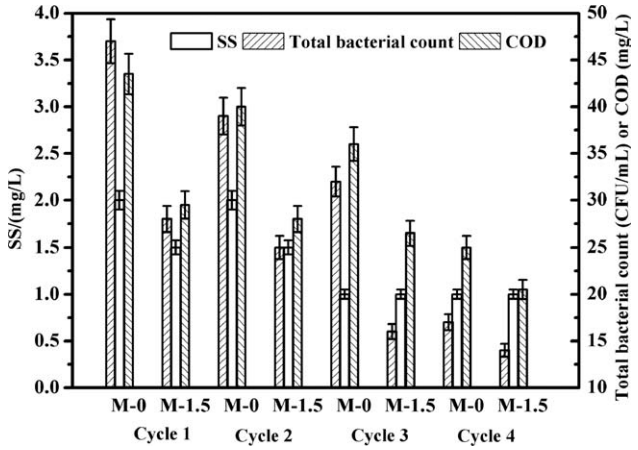

Figure 9. Water quality of the permeation water: the SS concentration in the feed water is 53 mg L^{-1}; the COD concentration in the feed water is 172.5 mg L^{-1}; the total bacterial count in the feed water is 435 CFU mL^{-1}; the filtration pressure is 0.1 MPa; and the temperature is 20°C ± 1°C.

membrane in contrast with the unmodified membrane (66 CFU mL^{-1}). Mostly, the outer cell-wall of the bacterium is the polysaccharide which is a hydrophobic substance.[41] As a result, bacteria tend to attach on the hydrophobic membrane surface. In other words, the bacteria are apt to be rinsed off from the hydrophilic membrane surface. Therefore, these results demonstrated that the membrane with nano-SiO_2 addition presented better property for preventing the *E. coli* attachment.

Supernatant Liquor Filtration Experiment. Figure 8 displays the results of the multi-cycle filtration operations with the supernatant liquor collected from a sedimentation tank of a municipal wastewater plant. The fluxes of both membranes presented a sharp decline during the filtration of the supernatant liquor. For the unmodified membrane, the flux decreased from 199 L m^{-2} h^{-1}(PWF) to 94 L m^{-2} h^{-1}, which declined sharper than that of the modified membrane. The initial fluxes in each cycle of the modified and unmodified membranes are likewise different. Specifically, the modified membrane exhibited more steady initial flux than the unmodified membrane throughout the four filtration cycles (Figure 8). Figure 8 also reveals that the permeability of the unmodified membrane was clearly influenced by the membrane fouling and could not recover as well as the modified membranes after the same rinsing steps.

The specific FRR and RFR values of the two kinds of membranes are summed up in the Table III. The pure water flux of the modified membrane could recovery its original value of 94.25% after simply physical backwashed, while that value of the unmodified membrane is only 84.10%. Both the FRR and the RFR values reveal that the membranes with the nano-SiO_2 addition presented better antifouling performance and flux recovery ratio.

Figure 9 presents the SS, total bacterial count and COD in the permeation water of the modified and unmodified membranes for the supernatant liquor filtration. The permeation water from the modified membrane exhibited a better effluent quality than that from the unmodified membrane, especially at the cycle 1. Specifically, the modified membranes presented good removal efficiencies of SS (over 97.2%), COD (up to 82.9%) and total bacteria (more than 93.6%). The SS content, COD content and total bacterial count were less than 1.5 mg L^{-1}, 29.5 mg L^{-1}, and 435 CFU mL^{-1}, respectively. But in the next filtration cycles, the retention ability of the unmodified membrane increased. This phenomenon might be interpreted as follows: The retention ability of a pure membrane mainly depended on its pore size at the beginning of the filtration (e.g., cycle 1). In the subsequent filtration cycles, there were some residual contaminants accumulated on the membrane surface, which diminished the membrane pore size and increased membrane filtration resistance. Therefore, it can be observed that all the membrane presented the improved retention ability (Figure 8) but declined permeation flux (Figure 8) with the prolonged filtration cycles. Even though both the modified and unmodified membranes showed excellent retention abilities to SS, COD and the bacteria at the cycle 4, the flux of the modified membrane was still much higher than the unmodified one.

Table III. Results of the Different Membranes' Antifouling Performance Evaluation

	RFR (%)					
	Cycle 1	Cycle 2	Cycle 3	Cycle 4	Average	FRR (%)
M-0	52.42	53.47	54.45	55.83	54.04	84.10
M-1.5	43.83	44.35	44.73	44.83	44.44	94.25

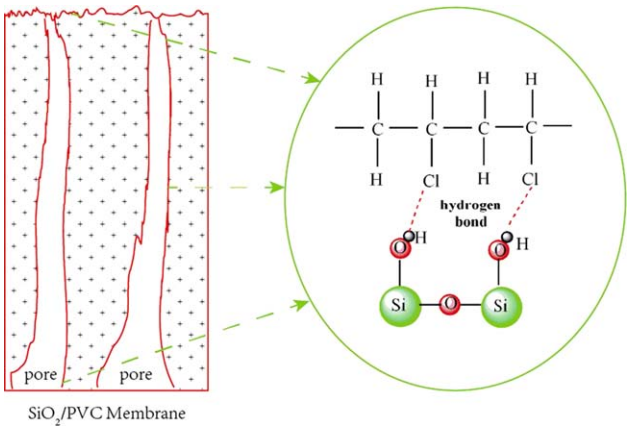

Figure 10. Schematic illustration of the antifouling mechanism of the modified membranes. [Color figure can be viewed in the online issue, which is available at wileyonlinelibrary.com.]

Thus, PVC membranes modified with nano-SiO_2 exhibit great applicable potential in the municipal wastewater treatment for their low cost, better antifouling performance, and higher removal efficiencies of SS, COD and total bacteria.

Antifouling Mechanism Analysis

As depicted in Figure 1(b), nano-SiO_2 particles presented excellent hydrophilicities for abundant —OH groups on their surface. When nano-SiO_2 particles added into the PVC casting solutions, they can be uniformly inlaid on the membrane's surface and pores (displayed in Figure 10). The —OH groups on the surface of SiO_2 particles interact with Cl atoms of PVC chains through hydrogen bonds. Thus, a hydrophilic layer was formed on the surface and the cross section of the modified membrane with the addition of nano-SiO_2. This hydrophilic layer can effectively prevent the hydrophobic substance (such as protein and bacterium) adsorption or attachment. In addition, when the membranes are used to filter the supernatant liquor, the hydrophobic contaminants together with SS could accumulate on the surface of the membranes and gradually form a cake layer, thereby leading to membrane fouling. However, the cake layer would probably remove from the hydrophilic surface through strong stirring and washing. That's the main reason for the modified membrane can keep better antifouling performance and higher flux recovery ratio.

CONCLUSIONS

In this study, we reported SiO_2 nanoparticle modified PVC membrane with novel properties, higher separation efficiencies, and greater industrial applications compared with unmodified membrane. Briefly, the following conclusions can be drawn:

1. With appropriate nano-SiO_2 addition, the hydrophilicities, mechanical properties and pure water fluxes of PVC-based membranes were significantly enhanced. However, the casting solutions with 3 wt % or higher nano-SiO_2 loading rate exhibited increased viscosities, unfavorable degassed effect and film-formation performance.
2. Compared with unmodified membrane, the membrane with dosage of 1.5 wt % nano-SiO_2 presented better abilities against the protein absorption and bacterial attachment, and better antifouling performance in the purification treatment of supernatant liquor from the secondary sedimentation tank.
3. The SiO_2/PVC membranes show great applicable potential in the municipal wastewater treatment for their low cost and high removal efficiencies of SS (over 97.2%), COD (up to 82.9%), and total bacteria (more than 93.6%).

ACKNOWLEDGMENTS

This work was supported by the National Natural Science Foundation of China (51108112), the Natural Science Foundation of Heilongjiang Province (E201252), Fundamental Research Funding of Harbin Engineering University (HEUFT06029), and Open Project of State Key Laboratory of Urban Water Resource and Environment, Harbin Institute of Technology (ESK201004).

REFERENCES

1. Howe, K. J.; Clark, M. M. *Environ. Sci. Technol.* **2002**, *36*, 3571.
2. Sofiah, H.; Nora'aini, A.; Msrinah, M. A. *J. Appl. Polym. Sci.* **2010**, *10*, 3325.
3. Liu, B. C.; Chen, C.; Zhang, W.; Crittenden, J.; Chen, Y. S. *Desalination* **2012**, *307*, 26.
4. Zhang, X. Z.; Chen, Y. S.; Konsowa, A. H.; Zhu, X. S.; Crittenden, J. C. *Sep. Purif. Technol.* **2009**, *70*, 71.
5. Xu, J. A.; Xu, Z. L. *J. Membr. Sci.* **2002**, *208*, 203.
6. Alsalhy, Q. F.; Rashid, K. T.; Noori, W. A.; Simone, S.; Figoli, A.; Drioli, E. *J. Appl. Polym. Sci.* **2012**, *124*, 2087.
7. Liu, H. L.; Xiao, C. F.; Huang, Q. L.; Hu, X. Y. *Desalination* **2013**, *331*, 35.
8. Zhu, X. Y.; Loo, H. E.; Bai, R. B. *J. Membr. Sci.* **2013**, *436*, 47.
9. Baker, R. W. Membrane Technology and Applications, 2nd ed.; Wiley: New York, **2004**.
10. Rana, D.; Matsuura, T. *Chem. Rev. (Washington, DC, U. S.)* **2010**, *110*, 2448.
11. Wang, P. P.; Ma, J.; Wang, Z. H.; Shi, F. M.; Liu, Q. L. *Langmuir* **2012**, *28*, 4776.
12. González Muñoza, M. P.; Navarroa, R.; Saucedoa, I.; Avilaa, M.; Prádanosb, P.; Palaciob, L.; Martínezb, F.; Martínb, A.; Hernándezb, A. *Desalination* **2006**, *191*, 273.
13. Lohokare, H. R.; Kumbharkar, S. C.; Bhole, Y. S.; Kharul, U. K. *J. Appl. Polym. Sci.* **2006**, *101*, 4378.
14. Mosqueda-Jimenez, D. B.; Narbaitz, R. M.; Matsuura, T. *J. Appl. Polym. Sci.* **2006**, *99*, 2978.
15. Meng, J. Q.; Li, J. H.; Zhang, Y. F.; Ma, S. N. *J. Membr. Sci.* **2014**, *455*, 405.
16. Huang, J.; Zhang, K. S.; Wang, K.; Xie, Z. L.; Ladewig, B.; Wang, H. T. *J. Membr. Sci.* **2012**, *423*, 362.
17. Zhao, S.; Wang, Z.; Wang, J. X.; Yang, S. B.; Wang, S. C. *J. Membr. Sci.* **2011**, *376*, 83.
18. Shen, J. N.; Yu, C. C.; Ruan, H. M.; Gao, C. J.; Van der Bruggen, B. *J. Membr. Sci.* **2013**, *442*, 18.
19. Chang, Q. B.; Zhou, J. E.; Wang, Y. Q.; Wang, J. M.; Meng, G. Y. *Desalination* **2010**, *262*, 110.

20. Pourjafar, S.; Rahimpour, A.; Jahanshahi, M. *J. Ind. Eng. Chem.* **2012**, *18*, 1398.
21. Wang, Q. Q.; Wang, X. T.; Wang, Z. H.; Huang, J.; Wang, Y. *J. Membr. Sci.* **2013**, *442*, 57.
22. Maximous, N.; Nakhla, G.; Wan, W.; Wong, K. *J. Membr. Sci.* **2010**, *352*, 222.
23. Ahmad, A. L.; Majid, M. A.; Ooi, B. S. *Desalination* **2011**, *268*, 266.
24. Yu, L. Y.; Xu, Z. L.; Shen, H. M.; Yang, H. *J. Membr. Sci.* **2009**, *337*, 257.
25. Shawky, H. A.; Chae, S. R.; Lin, S. H.; Wiesner, M. R. *Desalination* **2011**, *272*, 46.
26. Mansourpanah, Y.; Madaeni, S. S.; Rahimpour, A.; Adeli, M.; Hashemi, M. Y.; Moradian, M. R. *Desalination* **2011**, *277*, 171.
27. Liao, C. J.; Zhao, J. Q.; Yu, P.; Tong, H.; Luo, Y. B. *Desalination* **2012**, *285*, 117.
28. Ogoshi, T.; Chujo, Y. *J. Polym. Sci. A Polym. Chem.* **2005**, *43*, 3543.
29. Adams, L. K.; Lyon, D. Y.; Alvarez, Pedro J. J. *Water Res.* **2006**, *40*, 3527.
30. Jin, L. M.; Shi, W. X.; Yu, S. L.; Yi, X. S.; Sun, N.; Ma, C.; Liu, Y. S. *Desalination* **2012**, *298*, 34.
31. Yu, H. X.; Zhang, X. F.; Zhang, Y. T.; Liu, J. D.; Zhan, H. Q. *Desalination* **2013**, *326*, 69.
32. Basri, H.; Ismail, A. F.; Aziz, M. *Desalination* **2011**, *273*, 72.
33. Chen, X. R.; Su, Y.; Shen, F.; Wan, Y. H. *J. Membr. Sci.* **2011**, *384*, 44.
34. Venault, A.; Liu, Y. H.; Wu, J. R.; Yang, H. S.; Chang, Y.; Lai, J. Y.; Aimar, P. *J. Membr. Sci.* **2014**, *450*, 340.
35. Liang, S.; Xiao, K.; Mo, Y. H.; Huang, X. *J. Membr. Sci.* **2012**, *394*, 184.
36. Mei, S.; Xiao, C. F.; Hu, X. Y.; Shu, W. *Desalination* **2011**, *280*, 378.
37. Majeed, S.; Fierro1, D.; Buhr, K.; Wind, J.; Du, B.; Boschetti-de-Fierr, A.; Abetz, V. *Desalination* **2011**, *280*, 378.
38. Lu,Y.; Yu, S. L.; Chai, B. X.; Shun, X. D. *J. Membr. Sci.* **2006**, *276*, 162.
39. Chiag, Y. C.; Chang, Y.; Chen, W. Y.; Ruaan, R. C. *Langmuir* **2012**, *28*, 1399.
40. Zhao, C.; Li, X. S.; Li, L. Y.; Cheng, G.; Gong, X.; Zheng, J. *Langmuir* **2013**, *29*, 1517.
41. Lin, N. J.; Yang, H. S.; Chang, Y.; Tung, K. L.; Chen, W. H.; Cheng, H. W.; Hsiao, S. W.; Aimar, P.; Yamamoto, K.; Lai, J. Y. *Langmuir* **2013**, *29*, 10183.